BMB
Reports

BMB Rep. 2024; 57(6): 263-272
www.bmbreports.org

Invited Mini Review

Distinctive contribution of two additional residues in protein aggregation of Aβ42 and Aβ40 isoforms

*Dongjoon Im & Tae Su Choi**
Department of Life Sciences, Korea University, Seoul 02841, Korea

Amyloid-β (Aβ) is one of the amyloidogenic intrinsically disordered proteins (IDPs) that self-assemble to protein aggregates, incurring cell malfunction and cytotoxicity. While Aβ has been known to regulate multiple physiological functions, such as enhancing synaptic functions, aiding in the recovery of the blood-brain barrier/brain injury, and exhibiting tumor suppression/antimicrobial activities, the hydrophobicity of the primary structure promotes pathological aggregations that are closely associated with the onset of Alzheimer's disease (AD). Aβ proteins consist of multiple isoforms with 37-43 amino acid residues that are produced by the cleavage of amyloid-β precursor protein (APP). The hydrolytic products of APP are secreted to the extracellular regions of neuronal cells. Aβ 1-42 (Aβ42) and Aβ 1-40 (Aβ40) are dominant isoforms whose significance in AD pathogenesis has been highlighted in numerous studies to understand the molecular mechanism and develop AD diagnosis and therapeutic strategies. In this review, we focus on the differences between Aβ42 and Aβ40 in the molecular mechanism of amyloid aggregations mediated by the two additional residues (Ile41 and Ala42) of Aβ42. The current comprehension of Aβ42 and Aβ40 in AD progression is outlined, together with the structural features of Aβ42/Aβ40 amyloid fibrils, and the aggregation mechanisms of Aβ42/Aβ40. Furthermore, the impact of the heterogeneous distribution of Aβ isoforms during amyloid aggregations is discussed in the system mimicking the coexistence of Aβ42 and Aβ40 in human cerebrospinal fluid (CSF) and plasma. [BMB Reports 2024; 57(6): 263-272]

INTRODUCTION

Alzheimer's disease (AD) is one of the prevalent neurodegenerative disorders, and is primarily caused by the misfolding of amyloidogenic proteins (1). Globally, approximately 32.3 million individuals suffer from dementia by AD, while the United States alone spends around a trillion dollars annually on social and economic costs associated with AD patients (2). While the exact causes of AD remain unclear, the amyloid cascade hypothesis (ACH) has been widely investigated to elucidate the etiological mechanisms of AD mediated by amyloid-β (Aβ) proteins (3-5). The hypothesis states that the aggregation of Aβ proteins of which the unstructured monomeric forms are converted to insoluble amyloid fibrils is central to AD pathogenesis.

Unstructured Aβ proteins self-assemble in a range of protein aggregates, spanning from small oligomeric intermediates (< 10 nm) (6, 7) to larger amyloid fibrils (> 50 nm) (Fig. 1A) (8, 9). These aggregates with varying morphologies are characteristic of AD manifesting as amyloid plaques in the brain tissues of AD patients (10), while also highly cytotoxic, causing membrane disruption (11), neuronal dysfunction (12), mitochondrial dysfunction (13), and ultimately, cell death (14). Furthermore, amyloid fibrillation of Aβ in AD progression is synergistic with the pathological aggregation of microtubule-associated protein tau (Tau) (15, 16). Aβ fibrils accelerate fibrillar aggregation of Tau, resulting in the rapid spreading of neurotoxic Tau aggregates in the brain of AD patients (17-19). Such Aβ-mediated tau pathology mechanism follows either indirect pathways through the impact of Aβ fibrils on neuronal physiology or direct pathways through Aβ fibril-mediated heterotypic seeding of Tau (20). Since the onset and progression of AD is closely associated with Aβ aggregation, understanding the nature of Aβ aggregation at the molecular level has been crucial to develop diagnostic and therapeutic strategies of AD. Molecular behaviors of Aβ peptides originate from multiple isoforms with different length of the primary structures by the cleavages of N-terminal and C-terminal regions. Given that the general significance of Aβ in AD has been widely described in other perspectives and reviews, in the current mini-review, we focus intensively on recent molecular studies of pathogenic Aβ isoforms (i.e., Aβ 1-42 [Aβ42] and Aβ 1-40 [Aβ40]) that are indispensable biomarkers of AD diagnosis.

*Corresponding author. Tel: +82-2-3290-3413; Fax: +82-2-3290-4144; E-mail: choitaesu@korea.ac.kr

https://doi.org/10.5483/BMBRep.2024-0044

Received 20 March 2024, Revised 16 April 2024, Accepted 26 April 2024, Published online 2 May 2024

Keywords: Alzheimer's disease, Amyloid-β precursor protein, Biophysics, Neurodegeneration

ISSN: 1976-670X (electronic edition)
Copyright ⓒ 2024 by the The Korean Society for Biochemistry and Molecular Biology
This is an open-access article distributed under the terms of the Creative Commons Attribution Non-Commercial License (http://creativecommons.org/licenses/by-nc/4.0) which permits unrestricted non-commercial use, distribution, and reproduction in any medium, provided the original work is properly cited.

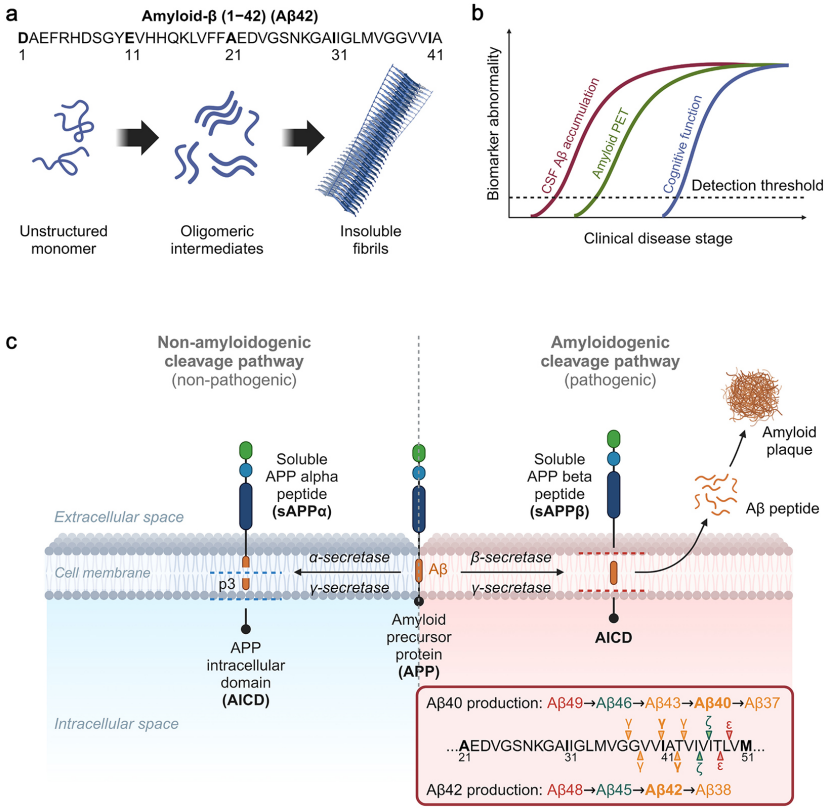

Fig. 1. Amyloid-β (Aβ) aggregation. (A) The primary structure of Aβ42 and aggregation mechanism of Aβ. Unstructured monomeric Aβ proteins self-assemble to oligomeric states; the oligomeric intermediates then elongate to insoluble fibrils. (B) Trajectories of Aβ biomarker abnormality and AD progression. Aβ as a biomarker can be assessed using cerebrospinal fluid Aβ and PET Aβ imaging. Aβ the panel image was adopted and reformatted from the review by Sperling *et al*. (26). (C) Enzymatic hydrolysis of amyloid-β precursor protein (APP) following non-pathogenic/pathogenic cleavage pathway. APP is sequentially cleaved by β-secretase and γ-secretase. As a result of the sequential cleavage, Aβ 1-42 (Aβ42) or Aβ 1-40 (Aβ40) is released to the extracellular space of neuronal cells. The inset of panel c shows the cleavage pathways of Aβ42/Aβ40 by γ-secretase.

IMPORTANCE OF Aβ42/40 RATIO AS A BIOMARKER OF AD

Quantitative analysis of Aβ42, phosphorylated Tau (pTau), and amyloid aggregate in clinical samples (e.g., human cerebrospinal fluid [CSF] (21, 22), plasma (23, 24), and amyloid plaque (25)), was utilized in the diagnosis of AD-mediated mild cognitive impairment (MCI) or dementia. Their significant association as a biomarker of AD was typically marked with the decrease of soluble species in fluid samples, and the increase of insoluble species in amyloid plaques of post-mortem patients. It has been suggested that an abnormality of a biomarker begins with the changes of Aβ concentrations in CSF and plasma (Fig. 1B) (26, 27); the change of the biomarker implies the accumulation of Aβ aggregates, thereby preceding the progression of AD. Using stable isotope labeling kinetics approach in conjunction with immunoprecipitation mass spectrometry, the quantitative analysis of Aβ isoforms was performed (28). The concentrations of Aβ42 in human plasma were found to be 30.13 pg/ml in the amyloid-positive group and 37.13 pg/ml in the control group. By contrast, Aβ40 concentrations of the amyloid-positive group were 272.4 pg/ml while those of the amyloid-negative group were 288.0 pg/ml. Likewise, in enzyme-linked immunosorbent assay (ELISA), the CSF levels of Aβ42 were 614.5 pg/ml (AD-MCI group) and 1,108 pg/ml (Control) while Aβ40 concentrations were 16,631 pg/ml (AD-MCI group) and 14,622 pg/ml (Control) (29). Thus, to improve the accuracy of the assessment for AD-mediated MCI and dementia, the Aβ42/Aβ40 ratio in human CSF (21) has been proposed as a new biomarker for AD. A growing body of evidence suggests that the diagnostic performance of the Aβ42/40 ratio in CSF is better than that of CSF in Aβ42 alone (22). Thus, when analyzing AD biomarkers in CSF, the measurement of relative Aβ42/40 ratio in CSF is currently widespread, rather than the absolute quantitation of Aβ42.

In addition to the diagnosis of amyloidosis in AD, the ratio

of Aβ42 to Aβ40 is utilized as one of the indices to monitor the therapeutic efficacy of antibodies in clinical trials of AD. The anti-amyloid antibody approach is one of the promising therapeutic strategies for Aβ clearance in human brain through passive immunotherapy. Aducanumab (Aduhelm) (30, 31), Lecanemab (Leqembi) (32), and Donanemab (TRAILBLAZER-ALZ 2) (33), approved or being examined by the US Food and Drug Administration (FDA), are human IgG1 monoclonal antibodies targeting Aβ aggregates. To monitor the progression of amyloid status during the administration of the antibodies to patients, Aβ42/40 ratios in human plasma or CSF are measured as supportive evidence of efficacy. As described, the ratio of Aβ42 to Aβ40 has recently been highlighted as an important biomarker of AD diagnosis and treatment. Thus, we discuss the origin of Aβ42 and Aβ40 secretion in the next section.

HETEROGENEITY OF Aβ ISOFORMS

Production of Aβ isoforms (Table 1) originates from the enzymatic cleavage of amyloid-β precursor protein (APP), yet the mechanism involved in determining the ratio of the isoforms remains unclear (34). The transmembrane domain of APP, which is embedded in the plasma membrane of human neuronal cells, contains multiple cleavage sites targeted by α-, β-, and γ-secretases (35). Orchestration of the secretases produces peptide fragments that are released into the extracellular space, involving neurotrophic activities, synaptic plasticity, and intracellular signaling (Fig. 1C) (36). The sequential cleavage of APP by β- and γ-secretases (i.e., amyloidogenic pathway) generates amyloidogenic Aβ peptides with 37-43 amino acid residues, whereas the combination of α- and γ-secretases guides the non-amyloidogenic secretion pathway that forms soluble P3 fragments. In the amyloidogenic secretion pathway, β-secretase generates soluble APP beta peptide (sAPPβ) and the APP C-terminal fragment (C99) by the cleavage of APP; then, γ-secretase splits C99 into the Aβ peptide and the APP intracellular domain (AICD). The length of Aβ proteins released to the extracellular region of neuronal cells typically terminates at either the Aβ40 or Aβ42 position, while AICD starts at the 49th or 50th position of C99. Although proteolytic cleavage mediated by the multiple secretases is the primary mechanism that determines the lengths of Aβ peptides, N-terminal truncated isoforms by non-conventional mechanisms (e.g., Cu^{II}-mediated self-hydrolysis, metalloproteases) have been reported as well (37). These isoforms share most of the primary structure with Aβ42 or Aβ40; however, the deletion of several N-terminal amino acid sequences significantly alter the aggregation behaviors of the truncated Aβ peptides.

Table 1. List of Aβ isoforms

Type of cleavage	Product
α-secretase (38)	17-X
β-secretase (39)	1-X/11-X
γ-secretase (40)	X-37/X-38/X-40/X-42/X-43/X-45/X-46/X-48/X-49
N-terminal truncation (41, 42)	2-X/3-X/4-X/8-X/9-X

The different locations of the cleavage sites in Aβ and AICD indicate that γ-secretase sequentially processes C99 at ε-cleavage (Aβ49 and 48), ξ-cleavage (Aβ46 and 45), and γ-cleavage (Aβ37, 38, 40, 42, and 43) sites. It has been proposed that Aβ40 production follows a tripeptide trimming pathway (Aβ49→46→43→40→37), while Aβ42 production follows a tri/tetrapeptide trimming pathway (Aβ48→45→42→38) (43, 44). The mechanism of the promiscuous hydrolysis by γ-secretase (45) remains unclear, but may involve structural dynamics/allosteric regulation of trimmed peptides affecting the sequential cleavages of C99 and the affinity of C-terminal motifs that determine the trimming pathways (46-48). Trimmed Aβ peptides are released from γ-secretase to the extracellular environment, when their interactions are destabilized. The two predominant forms of Aβ peptides are Aβ42 and Aβ40; Aβ42 is less abundant than Aβ40 (CSF Aβ40/Aβ42 = [9.6 ± 5.6] in normal control group, [14.2 ± 7.5] in patients with MCI, and [16.1 ± 6.7] in patients with AD) (49, 50). Aβ42 primarily leads to the formation of fibrillar aggregates, because the fibrillation rate of Aβ42 is much faster than that of Aβ40 (51, 52). Hence, the ratio of Aβ42 to Aβ40 in CSF and plasma is one of the common biomarkers to assess AD progression (22). A reduced Aβ42/Aβ40 ratio indicates the conversion of Aβ42 in CSF samples into aggregate species (53).

The presence of two additional C-terminal residues (Ile41 and Ala42) dramatically alters the aggregation propensity of Aβ42, compared to Aβ40. It is important to note that all Aβ isoforms are classified as intrinsically disordered proteins (IDPs), due to the lack of strong electrostatic/hydrophobic intramolecular interactions for a globular structure (51). Although the flexible conformations of Aβ42 and Aβ40 make them biophysically undistinguishable in the monomeric state, the slight difference at the C-terminus leads to significances in the aggregation kinetics and fibril structures of Aβ42 and Aβ40. This fact indicates that the structural dynamics of Aβ isoforms with the small change in the primary structures can influence the aggregation mechanism (54, 55). Hence, the impact of the two additional residues of Aβ42 should be emphasized to describe AD pathogenesis from the viewpoint of Aβ molecules. Thus, the molecular details of Aβ42 and Aβ40 in the aggregation are discussed in the next section.

CONFORMATIONAL FEATURES OF Aβ AMYLOID FIBRILS

It has been a challenging issue to determine what type of Aβ aggregates is central to neurotoxicity in AD, because the molecular mechanism and toxicology studies of Aβ aggregates (i.e., small oligomer, protofibrils, mature fibrils) indicated that the

neurotoxic Aβ species were not limited to a single form (56). Although extensive research has focused on understanding the assembly mechanisms and neurotoxic effects of Aβ aggregates during the last decades, our understanding of AD and Aβ aggregates has remained shallow. However, the recent advancements in immunotherapy targeting fibrillar Aβ aggregates have identified the importance of fibrillar Aβ aggregates as a main target to alleviate AD-mediated MCI and dementia (32). The fibrillar Aβ aggregates are deposited in the amyloid plaque, a pathological hallmark of AD present in the extracellular region of neuronal cells (57). The fibril structure of Aβ aggregates is composed of β-sheet rich, unbranched, unidirectional protein assemblies (58). The peptide backbone and side chains of Aβ monomers are tightly packed following the spine of the fibril structure, and the monomers in the spine are repeated at ~4.8 Å intervals (59). The peptide backbone of Aβ monomer forms intermolecular hydrogen bonds that strengthen β-sheet alignment. Stacking of aromatic/polar side chains and salt bridges of acidic/basic side chains further stabilizes the fibril structure through hydrophobic/electrostatic interactions and hydrogen bonds. A single stack of the fibril structure is defined as a protofibril, and multiple protofibril bundles are laterally assembled to a mature fibril. Lateral assemblies of the protofibrils are induced when the hydration shell surrounding the protofibril is liberated due to hydrophobic and electrostatic interactions between side chains on the fibril surface.

The fibril structures of Aβ42 and Aβ40 share the characteristics of non-covalent interactions due to the similarity of the fibril structure, yet different topological alignments are observed in the cross-section of the fibrils (Fig. 2). Cryo-electron microscopy (Cryo-EM) structures of Aβ42 fibrils extracted from the brain tissues of sporadic AD patients predominantly form Type I/II fibrils made of two identical S-shaped protofibrils (8). The β-sheet rich core region of the Type I protofibrils extends from Gly9 to Ala42 (Fig. 2A). The N-terminal arm (residues 9-18) and the S-shaped region (residues 19-42) constitute the cross section of the fibril spine of the Type I case. The interfacial spaces of the two protofibrils in the mature fibril are stabilized by tight packing of hydrophobic residues (Val, Leu, Phe) on the internal surface of the protofibril, while positive-

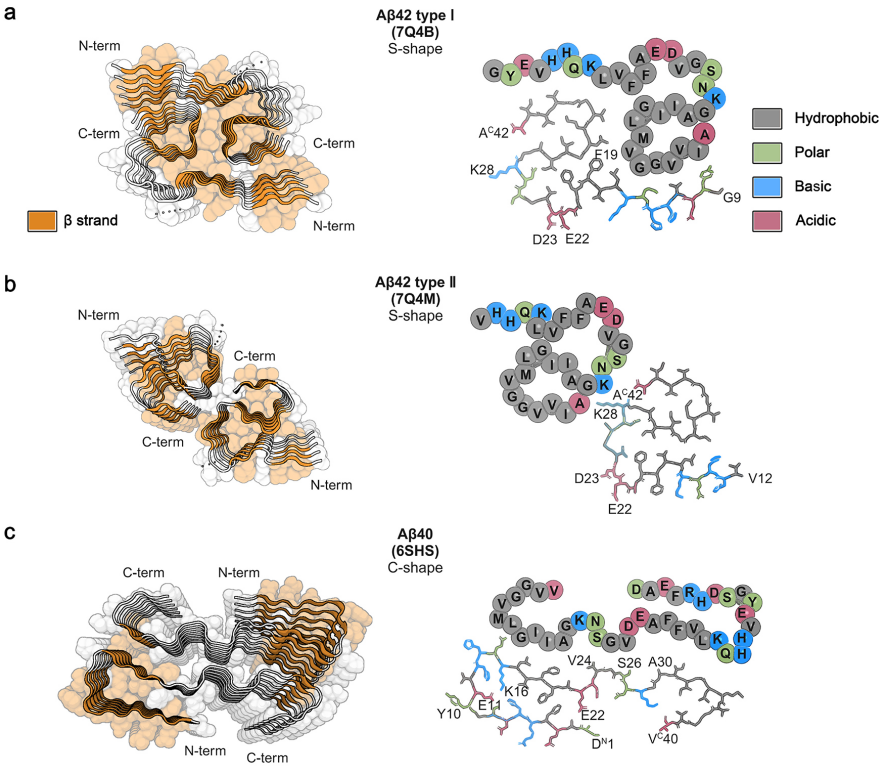

Fig. 2. Conformations of Aβ42 and Aβ40 fibrils. (A, B) Cryo-electron microscopy (cryo-EM) structures of (A) Type I and (B) Type II Aβ42 fibrils isolated from the brain tissues of sporadic and familial AD patients. The cross-sections of both Type I/II Aβ42 protofibrils are oriented as the S-shaped conformation, while the inter-fibrillar contact areas are not identical. (C) Cryo-EM structures of Aβ40 fibrils generated by seeding fresh Aβ40 with sonicated cortex tissue extract of an AD patient. Unlike Aβ42, the C-shaped conformation of Aβ40 is observed in the protofibril structure. The protofibrils of Aβ40 are in parallel alignment, forming the mature fibril structure. In the left panel, the β-sheet structures are highlighted in orange, while in the right panel, each amino acid is colored differently according to its polarity and charge state.

ly/negatively charged side chains (Glu, Lys, Asp) are oriented toward the outward direction on the fibril surface. The Type II protofibril structure extends from Val12 to Ala42 with four β-strands (Fig. 2B). The cross section of the spine is similar to the Type I structure with a shorter N-terminal arm. In addition, the interfaces between two S-shaped protofibrils are stabilized by salt bridges between the side chain of Lys28 and C-terminus of Ala42. Hydrophobic residues that are tightly packed in the interspace of protofibrils in Type I structure are exposed to the outside, forming a wide hydrophobic patch. The S-shape conformation of Aβ42 fibril structures is the common feature in other cryo-EM (60) and nuclear magnetic resonance (NMR) (58, 61, 62) structures of Aβ42.

In contrast to Aβ42 fibrils, the cryo-EM structure of Aβ40 fibrils extracted from the meninges of AD patients span the residues from Asp1 to Val40 (9). The topology of the Aβ40 protofibril adopts a C-shaped conformation with the N-/C-terminal arches (Fig. 2C). These arches fold toward the central hydrophobic domain, shielding the core region of the fibrils. Most of the positively/negatively charged side chains are solvent-exposed, except for Glu11 and Lys16 buried within the N-terminal arch, but stabilized through a salt bridge. Two protofibrils are contacted around ^{24}VGS^{26}, forming a cross-stack heterotypic zipper with two small cavities found in the overall structure of the mature fibril. The C-shaped conformation of the core region in Aβ40 fibrils is commonly observed in other solid-state NMR (63, 64) structures. The core residues shared in the C-shape extend from Tyr10 to Val40, and the hydrophobic residues (residues 30-40) involve the inter-protofibril interaction in the mature fibril. The topology of Aβ40 fibrils significantly differs from that of Aβ42 fibrils, but the Arctic mutation (E22G) (65) and the Osaka mutation (E22△) (66) allow Aβ40 to form Aβ42-like fibrils with the N-terminal arm and the S-shaped conformation. Although the effect of Glu22 mutation on the fibril topology has not yet been fully investigated, a repulsive charge-charge interaction of Glu22 and Asp23 may regulate the folding of the C-terminal hydrophobic residues of Aβ40. Another conformation reported as one of the Aβ40 fibril structures is a parallel alignment of two Aβ40 monomers stacked from Tyr10 to Val40 in cryo-EM analysis (67). The fibril structure with the parallel conformation was produced by seeding fresh Aβ40 using sonicated cortex tissue extract of an AD patient. In addition, recent cryo-EM structures have reported the parallel stacking of two Aβ40 monomers (68-70). The fibril structures of Aβ42 and Aβ40 vary in the cross section of the protofibril and the interfibrillar contact area of the protofibril, implying that the additional two residues regulate considerable changes in the aggregation processes. In the next section, the mechanistic changes of Aβ42 and Aβ40 fibrillation are reviewed with the kinetic modelling of protein aggregation.

FIBRILLATION MECHANISM OF Aβ42 AND Aβ40

As the topologies of Aβ42 and Aβ40 fibrils are differentiated, the fibrillations of the two isoforms follow their independent aggregation pathways. At the initial stage of the fibrillation, the fibrillation of amyloid proteins begins with the primary nucleation of protein monomers (Fig. 3A). The nuclei are then elongated to amyloid fibrils by capturing protein monomers. In addition to the primary nucleation/elongation steps, the secondary nucleation on the aggregate surface (major) and the fragmentation of elongated fibrils (minor) catalyze the proliferation of active nuclei, exponentially accelerating the fibrillation due to the positive feedback between the fibril formation of nuclei and the secondary nucleation on the fibril surface. Aβ42 and Aβ40 have been the subject of systematic investigation of the

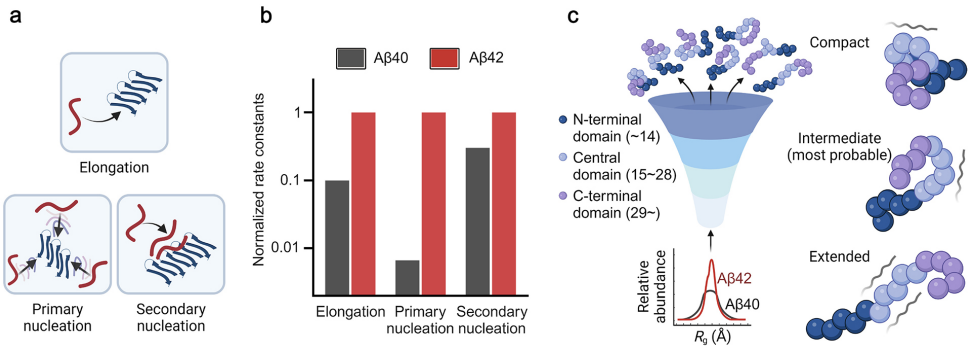

Fig. 3. Aggregation kinetics and structural dynamics of Aβ42 and Aβ40. (A) Schematic of the aggregation pathways that contribute the overall kinetics of Aβ: Primary nucleation, elongation, and secondary nucleation. (B) Relative aggregation rates of Aβ42 and Aβ40 in the primary nucleation, elongation, and secondary nucleation steps. The normalization of the rate constants was performed for each step. The rate constants of Aβ42 were set as a reference. The primary nucleation and elongation of Aβ42 are faster than those of Aβ40. Relative ratio of the secondary nucleation of Aβ42 to Aβ40 is in the range of the same magnitude. (C) Monomeric conformations of Aβ42 and Aβ40 that are involved in protein aggregation. In the structural pool of Aβ with wide distribution radius of gyration (R_g), representative features of aggregation-inducing conformers (Extended conformer in panel (C)) of Aβ42 show the exposed hydrophobic central regions, due to the intramolecular interaction of the C-terminal region.

aggregation process using the mechanistic models based on the primary/secondary nucleation, elongation, and fragmentation pathways (Fig. 3B). These microscopic pathways were demonstrated by mathematical modelling of *in situ* fibrillation kinetic traces in thioflavin T assay (71), a sensitive fluorescence dye to β-sheet rich assemblies (72). In the kinetic analysis (73), the primary nucleation of Aβ42 (3×10^{-4} M^{-2} s^{-1}) is 150-fold faster than that of Aβ40 (2×10^{-6} M^{-2} s^{-1}), while the elongation of Aβ42 (3×10^{6} M^{-1} s^{-1}) is 10-fold faster than that of Aβ40 (3×10^{5} M^{-1} s^{-1}). By contrast, the secondary nucleation of Aβ42 (1×10^{4} M^{-2} s^{-1}) is only 3-fold faster than that of Aβ40 (3×10^{3} M^{-2} s^{-1}). These results indicate that the two additional residues have a significant impact on the primary nucleation and the elongation, rather than on the secondary nucleation. The changes in the structural dynamics by the two hydrophobic side chains at the C-terminus of Aβ42 would be critical to reduce the activation energies of those molecular pathways. Thus, the molecular dynamics of Aβ42 and Aβ40 during the fibril growth are discussed in the next sections.

STRUCTURAL DYNAMICS AND PRIMARY NUCLEATION OF Aβ42 AND Aβ40 PEPTIDES

The self-assembly of Aβ monomers is guided by the structural transition of the proteins that promotes the conversion of intramolecular interaction to intermolecular interaction. This process leads to the formation of Aβ nuclei during the primary nucleation. The structural dynamics of Aβ42 and Aβ40 monomers have been thoroughly characterized through versatile biophysical approaches, such as two-dimensional infrared spectroscopy (2D-IR) (74), NMR spectroscopy (75), solution small-angle X-ray scattering (SAXS) (51), and molecular dynamics (MD) simulations (76). These approaches in common point out that (i) Aβ has weak intramolecular interactions, and (ii) the intermolecular hydrophobic interactions around residues 17-21 outcompete the intramolecular interactions, triggering the protein self-assembly above the threshold for spontaneous protein aggregation. The intramolecular interactions controlling the structural dynamics of Aβ are mediated by hydrophobic motifs within residues 10-35 (Fig. 3C). These hydrophobic motifs induce the formation of partially compact local structures by weak transient intramolecular interactions. Despite the flexible conformations of Aβ, local intramolecular interactions of Aβ in the central hydrophobic region delay the self-assembly of Aβ by intermolecular interactions. Compared to Aβ40 without Ile41 and Ala42, the C-terminus of Aβ42 disrupts the intramolecular interactions of the central region. The two additional residues preferably form a turn motif through frequent contacts with the hydrophobic region near residues 31-34 (75). This mode of action reduces the frequency of the intramolecular interactions that disturb the exposure of the core residues (Gln15-Gly25) and increases the possibility of intermolecular interactions in the core regions. If Ile41 and Ala42 are substituted to hydrophilic Asn residues at the same time, the hydrophilic variant of Aβ42 exhibits a slower aggregation rate, compared to the wild-type Aβ42 (77). Thus, the central hydrophobic regions of Aβ that are shielded by transient intramolecular hydrophobic interactions are attenuated in Aβ42. The hydrophobic effect of Ile41 and Ala42 also agrees well with the S-shaped conformation of Aβ42 fibrils being stabilized by the hydrophobic clusters in residues 30-42.

The nucleation of Aβ42 and Aβ40 is modulated by various environmental factors, such as pH (78), metal ions (79, 80), ionic strength, lipid membranes (81), small ligands (82, 83), peptides (76, 77), and proteins (84, 85). Because of the similarity of the primary structure, binding partners of Aβ42 and Aβ40 interact with similar regions, regardless of the two additional residues. Thus, the relative order of the nucleation rates (Aβ42 > Aβ40) is not affected. For example, the aggregation of Aβ peptides is promoted by lowering the pH in a neutral aqueous solution, because repulsive electrostatic interactions of Aβ peptides with negative charge states are attenuated by neutralization of total charge state through pH drop. However, the nucleation of Aβ42 is faster than that of Aβ40 regardless of pH changes, in that the C-terminal hydrophobic regions are not protonated/deprotonated. The increase of ionic strength shows a similar effect to the decrease of pH (86). As the ionic strength increases, the electrostatic repulsive interactions between Aβ peptides dissipate by stabilizing the charged side chains, and thereby, the nucleation rate increases.

The variation in aggregation kinetics of Aβ42 and Aβ40 is important to explain the benefit of a higher ratio of Aβ40 in human fluid that suppresses Aβ42 nucleation. Cross-interaction of different amyloid proteins is unconventional, due to the sequence-specificity in the tightly packed protein-protein interface of the aggregates. However, the similarity of Aβ42 and Aβ40 sequences enables the cross-interaction, facilitating hetero-oligomerization and fibrillation. Understanding the molecular behaviors of Aβ42 and Aβ40 when they coexist in a system has been challenging, because of the disordered protein structures and variable assembly states of Aβ. The average radius of gyration (R_g) distributions of Aβ42 (~20.6 Å) and Aβ40 (~20.1 Å) conformations in solution are similar (51). In the system where Aβ42 and Aβ40 coexist, Aβ40 competes with Aβ42 to form hetero-oligomers in the early stage of the aggregation, thus interfering with the self-assembly of Aβ42, and slowing the aggregation rate (73). Although the Aβ42 is more prone to aggregation in the monomeric state, Aβ40 effectively reduces the collision frequency of Aβ42 molecules, thereby delaying their self-assembly (51). Since two Aβ isoforms share the identical sequence from Asp1 to Val40, Aβ40-mediated suppression in the early stage of oligomerization would originate from the identical sequence. Molecular details of Aβ42-Aβ40 complexation remain elusive due to the structural flexibility and aggregation propensity of Aβ proteins. To overcome the limitation in the characterization of Aβ42-Aβ40 interactions, peptide design approaches mimicking the

sequence of Aβ and MD simulations would be a breakthrough for understanding the remaining question.

Other isoforms with shorter AA lengths (Aβ38/37) also delay the nucleation rate of the isoforms with longer AA lengths (54). Slowing the nucleation of Aβ42 by Aβ40 is beneficial to lowering the possibility of forming cytotoxic protein aggregates. Nevertheless, note that when Aβ42 coexists during the aggregation, the self-assembly of Aβ40 is accelerated (51). Accelerated fibrillation of Aβ40 indicates that Aβ42 aggregates behave as preformed nuclei, catalyzing the aggregation of Aβ40, despite the low aggregation propensity of Aβ40. Although Aβ40 aggregates are generally less cytotoxic than Aβ42 aggregates (87, 88), Aβ40 aggregates would induce the propagation of Aβ self-assembly (including Aβ42, Aβ40, Aβ38, Aβ37) by the elongation or the secondary nucleation process. Thus, the inhibitory effect of Aβ40 on Aβ42 aggregation is limited to the primary nucleation at the initial stage, and rather, Aβ40 participates in the overall aggregation.

The nucleation/elongation mechanism of Aβ under *in vitro* condition is not disturbed by regulatory mechanisms of neuroglial cells. However, in human brain, toxic Aβ species generated during fibrillation trigger the activation of neuroglial cells, initiating inflammatory responses and ultimately leading to cell death. This activation is initiated by the binding of Aβ aggregates to specific receptors (56, 89). Once activated, microglial cells migrate towards the plaques and engulf Aβ aggregates through phagocytosis (90, 91). The phagocytosis by the microglial cells is induced through the recognition of the Aβ aggregates by TAM receptors (92). Consequently, this process results in the formation of dense-core plaques and a reduction in toxic Aβ species, suppressing additional aggregation processes. Understanding these regulatory mechanisms by neuroglial cells would be essential for comprehending *in vivo* Aβ nucleation/elongation mechanisms and developing effective strategies to control AD progression.

CONCLUSION AND FUTURE PERSPECTIVES

Structural dynamics mediated by the additional hydrophobic side chains (Ile41 and Ala42) of Aβ42 (i) accelerates the nucleation and elongation steps, and (ii) induces the formation of an S-shaped fibril topology that is distinct from Aβ40. Since Aβ42 is more prone to aggregation than Aβ40, Aβ40 and shorter isoforms abundant in human fluids play a crucial role in the suppression of Aβ42 aggregation. If the ratio of Aβ42 was higher, the aggregation of Aβ42 would be severe due to the lack of inhibitory actions of the isoforms, and the aggregation of other Aβ isoforms would be promoted through the secondary nucleation by Aβ42 aggregates. Monitoring abnormal changes of Aβ42/40 ratio in AD diagnosis and therapeutic approach is correlated with the different aggregation propensities of Aβ42 and Aβ40. In addition to Aβ40, shorter Aβ isoforms (i.e., Aβ38, Aβ37) with low aggregation propensity are recently highlighted, due to their potential as novel biomarkers for AD diagnosis (50), and their inhibitory effects on Aβ42 aggregation (54). Given that the observation of the biomarker abnormalities in AD is highly relevant to the molecular role of Aβ isoforms, the molecular characterization of the shorter Aβ isoforms (amino acid length $<$ 42aa) and their formation mechanisms by γ-secretase would be crucial for future studies with regard to the ratio of short isoforms and Aβ42. Several familial mutations in AD cases involve the region of APP close to the cleavage sites of γ-secretase, thereby affecting the ratio of Aβ42 to Aβ40 (93-95). Due to the importance of γ-secretase activity, attempts have been made to reduce Aβ42 production using chemical modulators of γ-secretase. However, the modulation strategy of γ-secretase inevitably leads to side effects (e.g., cognitive deterioration), because the γ-secretase hydrolyzes other transmembrane proteins besides APP (96, 97). Thus, high specificity in the regulation of the enzymatic cleavage of APP would be required to develop the next generation of the γ-secretase modulator, to reduce the likelihood of side effects. Modulating γ-secretase activity may not be optimal to removing accumulated amyloid plaques but would be effective to maintain the low concentration of pathogenic Aβ isoforms in a subsequent therapeutic strategy.

In the context of a therapeutic strategy, regulation of Aβ42 aggregation at the molecular level, rather than Aβ40 or shorter isoforms, would be at the core of suppressing the initiation or propagation of Aβ deposition. The thermodynamic stability of Aβ42 aggregates is extremely high, despite the short distance of the primary sequence, compared to other amyloidogenic proteins (59). Such high stability of the fibril structure hinders the resolubilizing of the formed Aβ42 aggregates into a monomeric state while the aggregates propagate pathogenic aggregation through catalytic centers on the fibril surface. Hence, general strategies of the conventional Aβ42 inhibitors were limited to delaying the primary nucleation or isolating/depleting residual monomers to prevent additional aggregations. However, as shown in Fig. 1, the changes of biomarkers are not parallel with the onset of AD symptoms, implying that Aβ aggregates are already dominant in AD patients when the symptoms are observed in the late stage of AD. For this reason, passive immunization approaches using Aβ aggregate-targeting antibodies are focused on the activation of spontaneous fibril disaggregation/degradation by microglial cells. Thus, to facilitate the disaggregation/degradation pathways of Aβ aggregates by the antibodies, studies to overcome the thermodynamic stabilities of Aβ42 aggregates at the molecular level would be crucial.

ACKNOWLEDGEMENTS

This work was supported by the National Research Foundation of Korea (NRF) grant funded by the Korea government (MSIT) (No. RS-2023-00213155 and RS-2023-00221182 to T.S.C. & RS-2023-00274504 to D.I.), and the Korea Basic Science Institute (KBSI) National Research Facilities & Equipment Center

(NFEC) funded by the Korea government (Ministry of Education) (2019R1A6C1010028 to T.S.C.). Figures were created with Biorender.com and all graphics related to fibril structures were produced using PyMOL (98).

CONFLICTS OF INTEREST

The authors have no conflicting interests.

REFERENCES

1. No authors listed (2023) 2023 Alzheimer's disease facts and figures. Alzheimers Dement 19, 1598-1695
2. Gustavsson A, Norton N, Fast T et al (2023) Global estimates on the number of persons across the Alzheimer's disease continuum. Alzheimers Dement 19, 658-670
3. Kepp KP, Robakis NK, Høilund-Carlsen PF, Sensi SL and Vissel B (2023) The amyloid cascade hypothesis: an updated critical review. Brain 146, 3969-3990
4. Karran E, Mercken M and Strooper BD (2011) The amyloid cascade hypothesis for Alzheimer's disease: an appraisal for the development of therapeutics. Nat Rev Drug Discov 10, 698-712
5. Portugal Barron D and Guo Z (2024) The supersaturation perspective on the amyloid hypothesis. Chem Sci 15, 46-54
6. An J, Kim K, Lim HJ et al (2024) Early onset diagnosis in Alzheimer's disease patients via amyloid-β oligomers-sensing probe in cerebrospinal fluid. Nat Commun 15, 1004
7. Ashe KH (2020) The biogenesis and biology of amyloid beta oligomers in the brain. Alzheimers Dement 16, 1561-1567
8. Yang Y, Arseni D, Zhang W et al (2022) Cryo-EM structures of amyloid-β 42 filaments from human brains. Science 375, 167-172
9. Kollmer M, Close W, Funk L et al (2019) Cryo-EM structure and polymorphism of Aβ amyloid fibrils purified from Alzheimer's brain tissue. Nat Commun 10, 4760
10. Querol-Vilaseca M, Colom-Cadena M, Pegueroles J et al (2019) Nanoscale structure of amyloid-β plaques in Alzheimer's disease. Sci Rep 9, 5181
11. Viles JH (2023) Imaging amyloid-β membrane interactions: ion-channel pores and lipid-bilayer permeability in Alzheimer's disease. Angew Chem Int Ed 62, e202215785
12. Palop JJ and Mucke L (2010) Amyloid-β-induced neuronal dysfunction in Alzheimer's disease: from synapses toward neural networks. Nat Neurosci 13, 812-818
13. Naia L, Shimozawa M, Bereczki E et al (2023) Mitochondrial hypermetabolism precedes impaired autophagy and synaptic disorganization in App knock-in Alzheimer mouse models. Mol Psychiatry 28, 3966-3981
14. Calvo-Rodriguez M, Hou SS, Snyder AC et al (2020) Increased mitochondrial calcium levels associated with neuronal death in a mouse model of Alzheimer's disease. Nat Commun 11, 2146
15. Wang L, Benzinger TL, Su Y et al (2016) Evaluation of tau imaging in staging alzheimer disease and revealing interactions between β-amyloid and tauopathy. JAMA Neurol 73, 1070-1077
16. Le LTHL, Lee J, Im D et al (2023) Self-aggregating tau fragments recapitulate pathologic phenotypes and neurotoxicity of Alzheimer's disease in mice. Adv Sci 10, 2302035
17. He Z, Guo JL, McBride JD et al (2018) Amyloid-β plaques enhance Alzheimer's brain tau-seeded pathologies by facilitating neuritic plaque tau aggregation. Nat Med 24, 29-38
18. Lewis J, Dickson DW, Lin WL et al (2001) Enhanced neurofibrillary degeneration in transgenic mice expressing mutant tau and APP. Science 293, 1487-1491
19. Götz J, Chen F, van Dorpe J and Nitsch RM (2001) Formation of neurofibrillary tangles in P301L tau transgenic mice induced by Aβ42 fibrils. Science 293, 1491-1495
20. Busche MA and Hyman BT (2020) Synergy between amyloid-β and tau in Alzheimer's disease. Nat Neurosci 23, 1183-1193
21. Hansson O, Lehmann S, Otto M, Zetterberg H and Lewczuk P (2019) Advantages and disadvantages of the use of the CSF Amyloid β (Aβ) 42/40 ratio in the diagnosis of Alzheimer's disease. Alzheimer's Res Ther 11, 34
22. Delaby C, Estellés T, Zhu N et al (2022) The Aβ1-42/Aβ1-40 ratio in CSF is more strongly associated to tau markers and clinical progression than Aβ1-42 alone. Alzheimer's Res Ther 14, 20
23. Leuzy A, Mattsson-Carlgren N, Palmqvist S, Janelidze S, Dage JL and Hansson O (2022) Blood-based biomarkers for Alzheimer's disease. EMBO Mol Med 14, e14408
24. Brand AL, Lawler PE, Bollinger JG et al (2022) The performance of plasma amyloid beta measurements in identifying amyloid plaques in Alzheimer's disease: a literature review. Alzheimers Res Ther 14, 195
25. Chapleau M, Iaccarino L, Soleimani-Meigooni D and Rabinovici GD (2022) The role of amyloid PET in imaging neurodegenerative disorders: a review. J Nucl Med 63, S13-S19
26. Sperling RA, Aisen PS, Beckett LA et al (2011) Toward defining the preclinical stages of Alzheimer's disease: recommendations from the national institute on aging-Alzheimer's association workgroups on diagnostic guidelines for Alzheimer's disease. Alzheimers Dement 7, 280-292
27. Hansson O (2021) Biomarkers for neurodegenerative diseases. Nat Med 27, 954-963
28. Ovod V, Ramsey KN, Mawuenyega KG et al (2017) Amyloid β concentrations and stable isotope labeling kinetics of human plasma specific to central nervous system amyloidosis. Alzheimers Dement 13, 841-849
29. Lewczuk P, Lelental N, Spitzer P, Maler JM and Kornhuber J (2015) Amyloid-β 42/40 cerebrospinal fluid concentration ratio in the diagnostics of Alzheimer's disease: validation of two novel assays. J Alzheimer's Dis 43, 183-191
30. Sevigny J, Chiao P, Bussière T et al (2016) The antibody aducanumab reduces Aβ plaques in Alzheimer's disease. Nature 537, 50-56
31. Cummings J, Aisen P, Apostolova LG, Atri A, Salloway S and Weiner M (2021) Aducanumab: appropriate use recommendations. J Prev Alzheimers Dis 8, 398-410
32. van Dyck CH, Swanson CJ, Aisen P et al (2022) Lecanemab in early Alzheimer's disease. N Engl J Med 388, 9-21

33. Sims JR, Zimmer JA, Evans CD et al (2023) Donanemab in early symptomatic Alzheimer disease: the TRAILBLAZER-ALZ 2 randomized clinical trial. JAMA 330, 512-527
34. Müller UC, Deller T and Korte M (2017) Not just amyloid: physiological functions of the amyloid precursor protein family. Nat Rev Neurosci 18, 281-298
35. O'Brien RJ and Wong PC (2011) Amyloid precursor protein processing and Alzheimer's disease. Annu Rev Neurosci 34, 185-204
36. Brothers HM, Gosztyla ML and Robinson SR (2018) The physiological roles of amyloid-β peptide hint at new ways to treat Alzheimer's disease. Front Aging Neurosci 10, 118
37. Kummer MP and Heneka MT (2014) Truncated and modified amyloid-beta species. Alzheimer's Res Ther 6, 28
38. Esch FS, Keim PS, Beattie EC et al (1990) Cleavage of amyloid β peptide during constitutive processing of its precursor. Science 248, 1122-1124
39. Vassar R, Bennett BD, Babu-Khan S et al (1999) β-secretase cleavage of Alzheimer's amyloid precursor protein by the transmembrane aspartic protease BACE. Science 286, 735-741
40. De Strooper B, Annaert W, Cupers P et al (1999) A presenilin-1-dependent γ-secretase-like protease mediates release of Notch intracellular domain. Nature 398, 518-522
41. Masters CL, Simms G, Weinman NA, Multhaup G, McDonald BL and Beyreuther K (1985) Amyloid plaque core protein in Alzheimer disease and Down syndrome. Proc Natl Acad Sci U S A 82, 4245-4249
42. Wiltfang J, Esselmann H, Cupers P et al (2001) Elevation of β-amyloid peptide in sporadic and familial Alzheimer's disease and its generation in PS1 knockout cells. J Biol Chem 276, 42645-42657
43. Takami M, Nagashima Y, Sano Y et al (2009) γ-secretase: successive tripeptide and tetrapeptide release from the transmembrane domain of β-carboxyl terminal fragment. J Neurosci 29, 13042-13052
44. Qi-Takahara Y, Morishima-Kawashima M, Tanimura Y et al (2005) Longer forms of amyloid β protein: implications for the mechanism of intramembrane cleavage by γ-secretase. J Neurosci 25, 436-445
45. Wolfe MS (2019) Structure and function of the γ-secretase complex. Biochemistry 58, 2953-2966
46. Lee JY, Feng Z, Xie XQ and Bahar I (2017) Allosteric modulation of intact gamma-secretase structural dynamics. Biophys J 113, 2634-2649
47. Bhattarai A, Devkota S, Do HN et al (2022) Mechanism of tripeptide trimming of amyloid β-peptide 49 by γ-secretase. J Am Chem Soc 144, 6215-6226
48. Petit D, Hitzenberger M, Lismont S et al (2019) Extracellular interface between APP and Nicastrin regulates Abeta length and response to gamma-secretase modulators. EMBO J 38, e101494
49. Hellstrom-Lindahl E, Viitanen M and Marutle A (2009) Comparison of Abeta levels in the brain of familial and sporadic Alzheimer's disease. Neurochem Int 55, 243-252
50. Liu L, Lauro BM, He A et al (2023) Identification of the Aβ37/42 peptide ratio in CSF as an improved Aβ biomarker for Alzheimer's disease. Alzheimers Dement 19, 79-96
51. Heo CE, Choi TS and Kim HI (2018) Competitive homo- and hetero- self-assembly of amyloid-β 1-42 and 1-40 in the early stage of fibrillation. Int J Mass Spectrom 428, 15-21
52. Kuperstein I, Broersen K, Benilova I et al (2010) Neurotoxicity of Alzheimer's disease Abeta peptides is induced by small changes in the Abeta42 to Abeta40 ratio. EMBO J 29, 3408-3420
53. Gravina SA, Ho L, Eckman CB et al (1995) Amyloid-β Protein (Aβ) in Alzheimeri's disease brain: biochemical and immunocytochemical analysis with antibodies specific for forms ending at Aβ40 OR Aβ42(43). J Biol Chem 270, 7013-7016
54. Braun GA, Dear AJ, Sanagavarapu K, Zetterberg H and Linse S (2022) Amyloid-β peptide 37, 38 and 40 individually and cooperatively inhibit amyloid-β 42 aggregation. Chem Sci 13, 2423-2439
55. Jäkel L, Biemans EALM, Klijn CJM, Kuiperij HB and Verbeek MM (2020) Reduced influence of apoE on Aβ43 aggregation and reduced vascular Aβ43 toxicity as compared with Aβ40 and Aβ42. Mol Neurobiol 57, 2131-2141
56. Hampel H, Hardy J, Blennow K et al (2021) The amyloid-β pathway in Alzheimer's disease. Mol Psychiatry 26, 5481-5503
57. Rahman MM and Lendel C (2021) Extracellular protein components of amyloid plaques and their roles in Alzheimer's disease pathology. Mol Neurodegener 16, 59
58. Xiao Y, Ma B, McElheny D et al (2015) Aβ(1-42) fibril structure illuminates self-recognition and replication of amyloid in Alzheimer's disease. Nat Struct Mol Biol 22, 499-505
59. Sawaya MR, Hughes MP, Rodriguez JA, Riek R and Eisenberg DS (2021) The expanding amyloid family: structure, stability, function, and pathogenesis. Cell 184, 4857-4873
60. Gremer L, Schölzel D, Schenk C et al (2017) Fibril structure of amyloid-β(1-42) by cryo-electron microscopy. Science 358, 116-119
61. Wälti MA, Ravotti F, Arai H et al (2016) Atomic-resolution structure of a disease-relevant Aβ(1-42) amyloid fibril. Proc Natl Acad Sci U S A 113, E4976-E4984
62. Colvin MT, Silvers R, Ni QZ et al (2016) Atomic resolution structure of monomorphic Aβ42 amyloid fibrils. J Am Chem Soc 138, 9663-9674
63. Cerofolini L, Ravera E, Bologna S et al (2020) Mixing Aβ (1-40) and Aβ(1-42) peptides generates unique amyloid fibrils. Chem Commun 56, 8830-8833
64. Paravastu AK, Leapman RD, Yau WM and Tycko R (2008) Molecular structural basis for polymorphism in Alzheimer's β-amyloid fibrils. Proc Natl Acad Sci U S A 105, 18349-18354
65. Zielinski M, Peralta Reyes FS, Gremer L et al (2023) Cryo-EM of Aβ fibrils from mouse models find tg-APP-ArcSwe fibrils resemble those found in patients with sporadic Alzheimer's disease. Nat Neurosci 26, 2073-2080
66. Schütz AK, Vagt T, Huber M et al (2015) Atomic-resolution three-dimensional structure of amyloid β fibrils bearing the Osaka mutation. Angew Chem Int Ed 54, 331-335
67. Ghosh U, Thurber KR, Yau WM and Tycko R (2021) Molecular structure of a prevalent amyloid-β fibril polymorph from Alzheimer's disease brain tissue. Proc Natl

Acad Sci U S A 118, e2023089118
68. Frieg B, Han M, Giller K et al (2024) Cryo-EM structures of lipidic fibrils of amyloid-β (1-40). Nat Commun 15, 1297
69. Pfeiffer PB, Ugrina M, Schwierz N, Sigurdson CJ, Schmidt M and Fändrich M (2024) Cryo-EM analysis of the effect of seeding with brain-derived Aβ amyloid fibrils. J Mol Biol 436, 168422
70. Yang Y, Murzin AG, Peak-Chew S et al (2023) Cryo-EM structures of Aβ40 filaments from the leptomeninges of individuals with Alzheimer's disease and cerebral amyloid angiopathy. Acta Neuropathol Commun 11, 191
71. Meisl G, Kirkegaard JB, Arosio P et al (2016) Molecular mechanisms of protein aggregation from global fitting of kinetic models. Nat Protoc 11, 252-272
72. Wolfe LS, Calabrese MF, Nath A, Blaho DV, Miranker AD and Xiong Y (2010) Protein-induced photophysical changes to the amyloid indicator dye thioflavin T. Proc Natl Acad Sci U S A 107, 16863-16868
73. Meisl G, Yang X, Hellstrand E et al (2014) Differences in nucleation behavior underlie the contrasting aggregation kinetics of the Aβ40 and Aβ42 peptides. Proc Natl Acad Sci U S A 111, 9384-9389
74. Zhuang W, Sgourakis NG, Li Z, Garcia AE and Mukamel S (2010) Discriminating early stage Aβ42 monomer structures using chirality-induced 2DIR spectroscopy in a simulation study. Proc Natl Acad Sci U S A 107, 15687-15692
75. Yan Y and Wang C (2006) Aβ42 is more rigid than Aβ40 at the C terminus: implications for Aβ aggregation and toxicity. J Mol Biol 364, 853-862
76. Im D, Heo CE, Son MK, Park CR, Kim HI and Choi JM (2022) Kinetic Modulation of Amyloid-β (1-42) aggregation and toxicity by structure-based rational design. J Am Chem Soc 144, 1603-1611
77. Im D, Kim S, Yoon G et al (2023) Decoding the roles of amyloid-β (1-42)'s key oligomerization domains toward designing epitope-specific aggregation inhibitors. JACS Au 3, 1065-1075
78. Tian Y and Viles JH (2022) pH dependence of amyloid-β fibril assembly kinetics: unravelling the microscopic molecular processes. Angew Chem Int Ed 61, e202210675
79. Suh JM, Kim M, Yoo J, Han J, Paulina C and Lim MH (2023) Intercommunication between metal ions and amyloidogenic peptides or proteins in protein misfolding disorders. Coord Chem Rev 478, 214978
80. Yi Y and Lim MH (2023) Current understanding of metal-dependent amyloid-β aggregation and toxicity. RSC Chem Biol 4, 121-131
81. Heo CE, Park CR and Kim HI (2021) Effect of packing density of lipid vesicles on the Aβ42 fibril polymorphism. Chem Phys Lipids 236, 105073
82. Kim S, Hyun DG, Nam Y et al (2023) Genipin and pyrogallol: two natural small molecules targeting the modulation of disordered proteins in Alzheimer's disease. Biomed Pharmacother 168, 115770
83. Hyung SJ, DeToma AS, Brender JR et al (2013) Insights into antiamyloidogenic properties of the green tea extract (−)-epigallocatechin-3-gallate toward metal-associated amyloid-β species. Proc Natl Acad Sci U S A 110, 3743-3748
84. Yi Y, Lee J and Lim MH (2024) Amyloid-β-interacting proteins in peripheral fluids of Alzheimer's disease. Trends Chem 6, 128-143
85. Choi TS, Lee HJ, Han JY, Lim MH and Kim HI (2017) Molecular insights into human serum albumin as a receptor of amyloid-β in the extracellular region. J Am Chem Soc 139, 15437-15445
86. Yang X, Meisl G, Frohm B, Thulin E, Knowles TPJ and Linse S (2018) On the role of sidechain size and charge in the aggregation of Aβ42 with familial mutations. Proc Natl Acad Sci U S A 115, E5849-E5858
87. Quartey MO, Nyarko JNK, Maley JM et al (2021) The Aβ(1-38) peptide is a negative regulator of the Aβ(1-42) peptide implicated in Alzheimer disease progression. Sci Rep 11, 431
88. Moore BD, Martin J, de Mena L et al (2017) Short Aβ peptides attenuate Aβ42 toxicity in vivo. J Exp Med 215, 283-301
89. Lasagna-Reeves CA and Kayed R (2011) Astrocytes contain amyloid-β annular protofibrils in Alzheimer's disease brains. FEBS Lett 585, 3052-3057
90. Baik SH, Kang S, Son SM and Mook-Jung I (2016) Microglia contributes to plaque growth by cell death due to uptake of amyloid β in the brain of Alzheimer's disease mouse model. Glia 64, 2274-2290
91. Bolmont T, Haiss F, Eicke D et al (2008) Dynamics of the microglial/amyloid interaction indicate a role in plaque maintenance. J Neurosci 28, 4283-4292
92. Huang Y, Happonen KE, Burrola PG et al (2021) Microglia use TAM receptors to detect and engulf amyloid β plaques. Nat Immunol 22, 586-594
93. Suzuki N, Cheung TT, Cai XD et al (1994) An increased percentage of long amyloid β protein secreted by familial amyloid β protein precursor (βApp717) mutants. Science 264, 1336-1340
94. De Jonghe C, Esselens C, Kumar-Singh S et al (2001) Pathogenic APP mutations near the γ-secretase cleavage site differentially affect Aβ secretion and APP C-terminal fragment stability. Hum Mol Genet 10, 1665-1671
95. Lichtenthaler SF, Ida N, Multhaup G, Masters CL and Beyreuther K (1997) Mutations in the transmembrane domain of APP altering γ-secretase specificity. Biochemistry 36, 15396-15403
96. Coric V, Salloway S, van Dyck CH et al (2015) Targeting prodromal Alzheimer disease with avagacestat: a randomized clinical trial. JAMA Neurol 72, 1324-1333
97. Doody RS, Raman R, Farlow M et al (2013) A phase 3 trial of semagacestat for treatment of Alzheimer's disease. N Engl J Med 369, 341-350
98. Schrödinger (2021) The PyMOL Molecular Graphics System v. 2.5.